IV. Energy Deposition in the Detector and Spectrum Formation

a) charged particles

Bethe-Bloch formula

$$-\frac{dE}{dx} = \frac{4\pi q_e^4}{m_0}\frac{z^2}{v^2}\cdot NZ\cdot\left[\ln\frac{2m_0v^2}{I} - \ln\left(1-\beta^2\right) - \beta^2\right]$$

z, v: atomic number and velocity of projectile

N, Z: particle density and atomic number of absorber

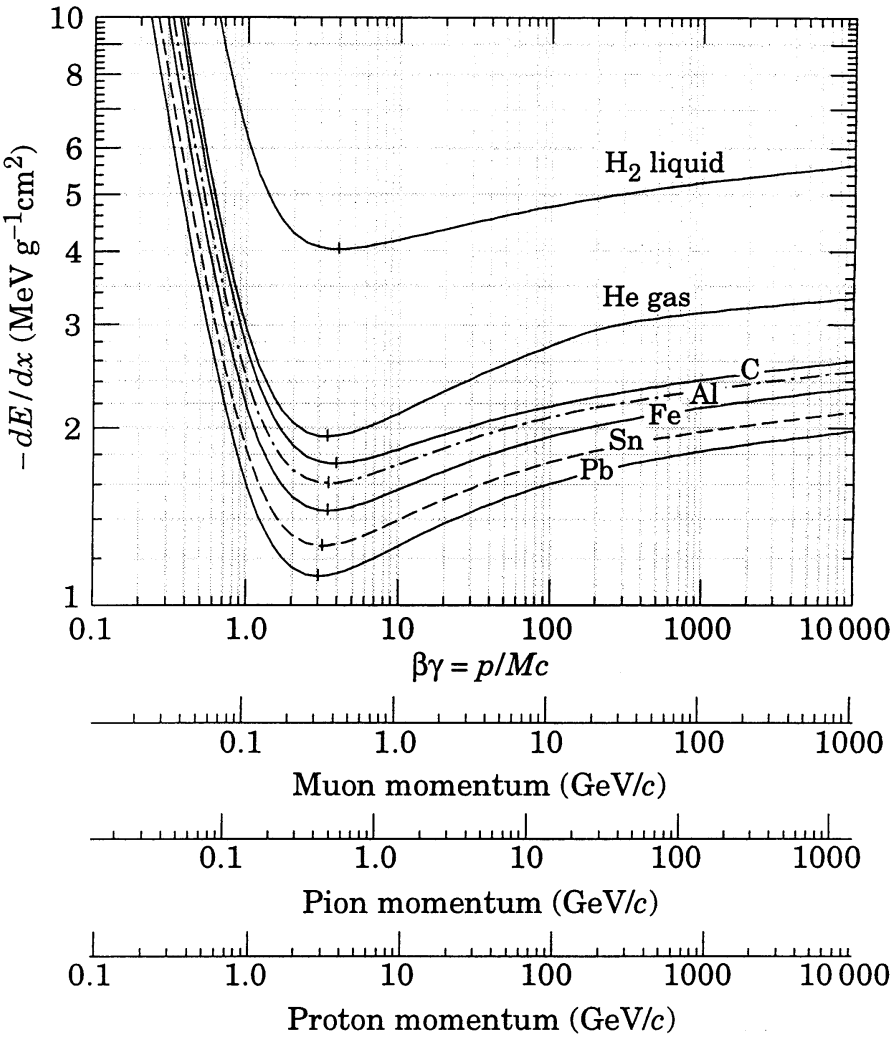

At $\beta\gamma \approx 3$ the differential energy loss assumes a minimum (minimum ionizing particles), independent of absorber.

dE/dx vs. E of protons in silicon

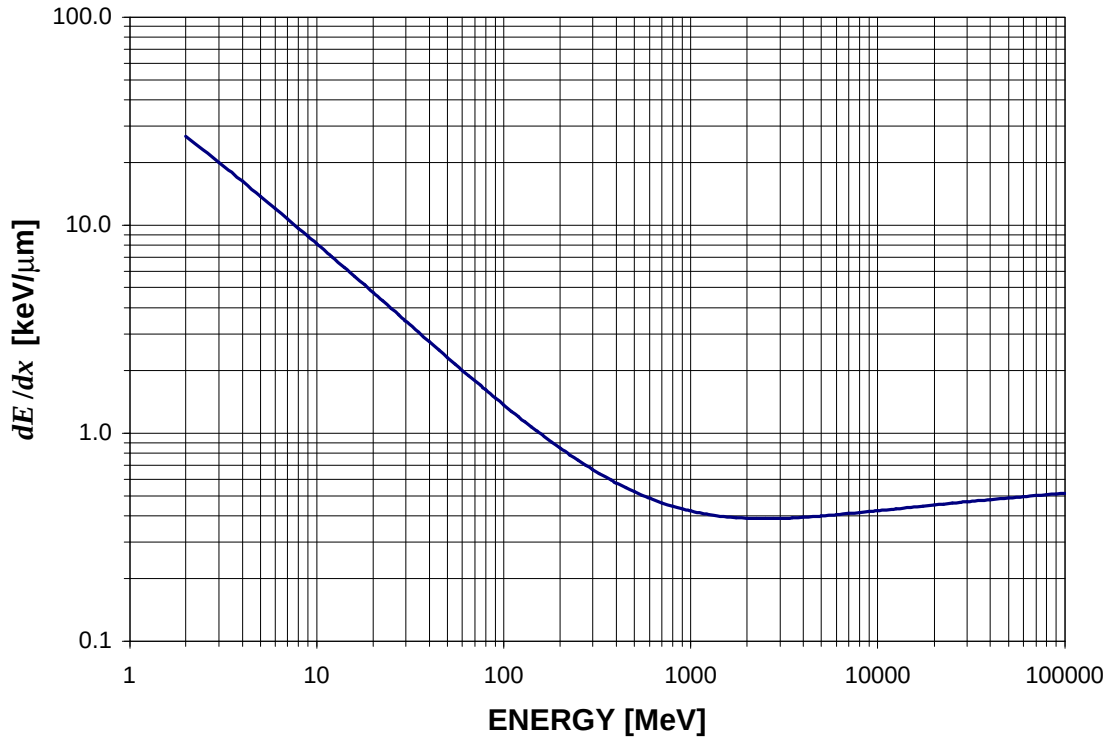

minimum ionization at 2 – 3 GeV

dE/dx vs. E of electrons in silicon

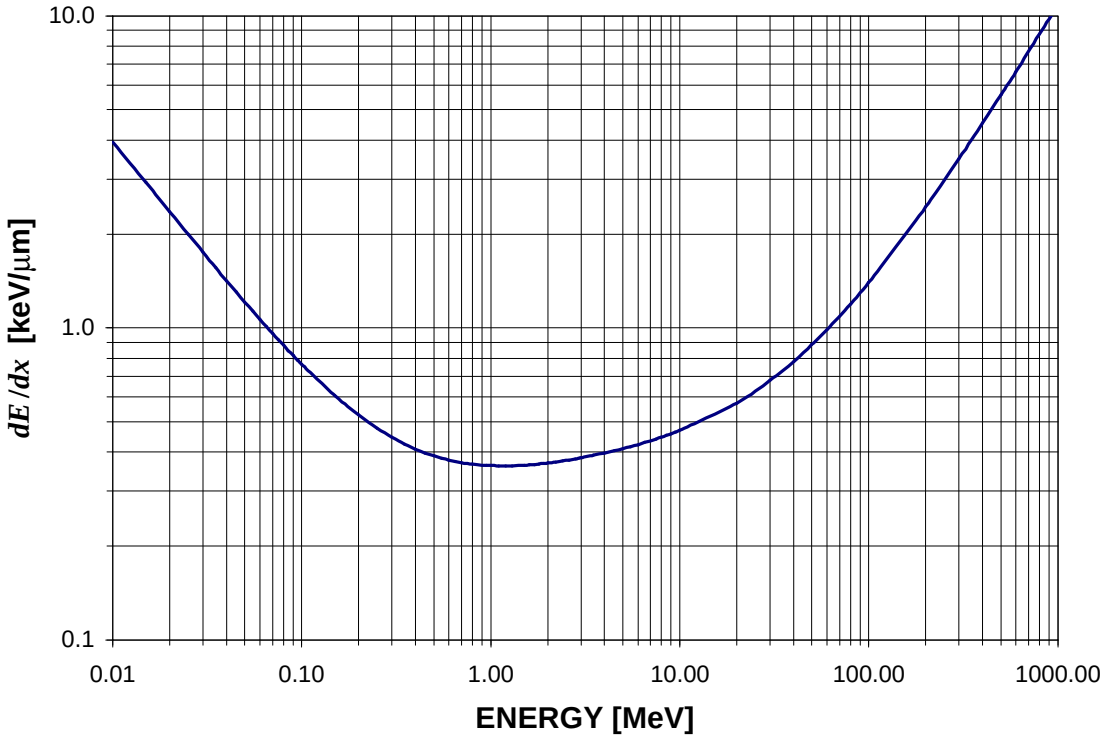

Minimum ionization at ~1 MeV.

At electron energies >50 MeV radiative energy loss dominates, so the stopping power increases more rapidly beyond the energy of minimum ionization than for protons.

For small velocities ($\beta << 1$)

$$-\frac{dE}{dx} \propto \left(\frac{z}{v}\right)^2 \cdot NZ$$

$\Rightarrow$ dE/dx increases with projectile charge squared
decreases with increasing projectile energy (v^2)

increases with target atomic number and density

dE/dx for alpha particles in various materials

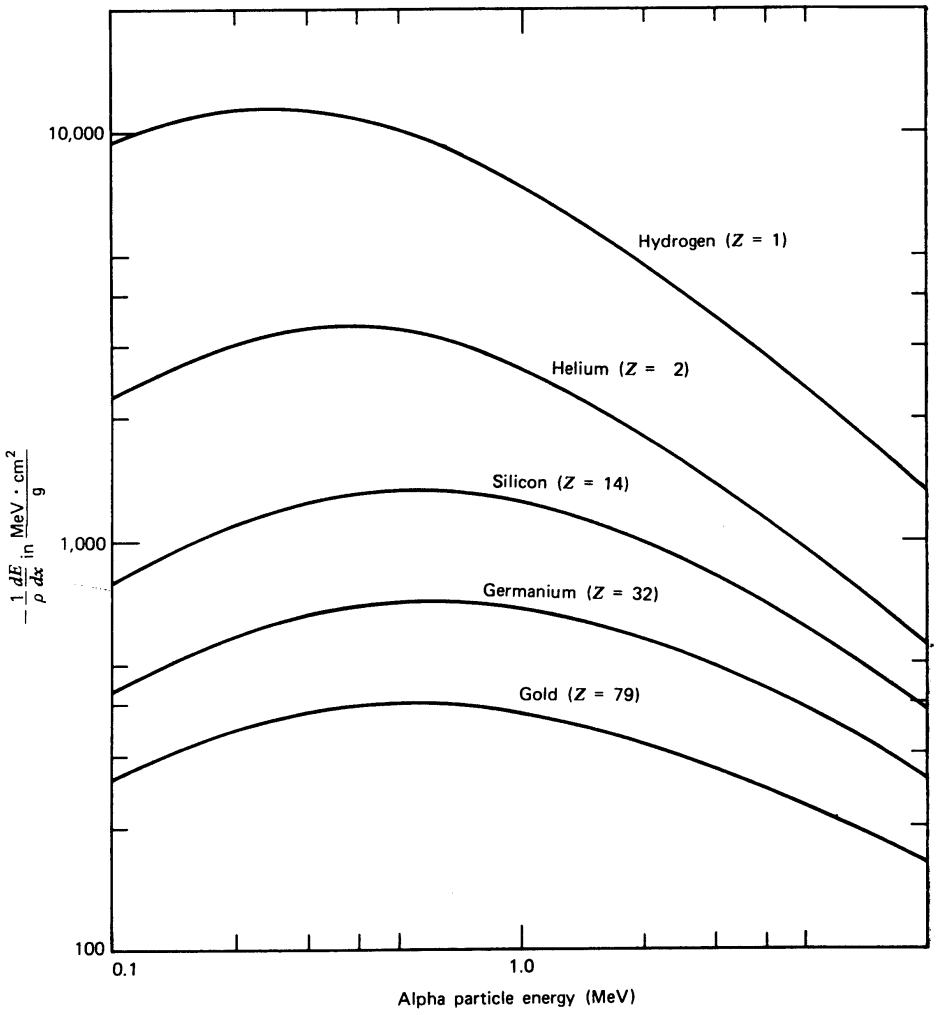

dE/dx vs. E for various charged particles in Si

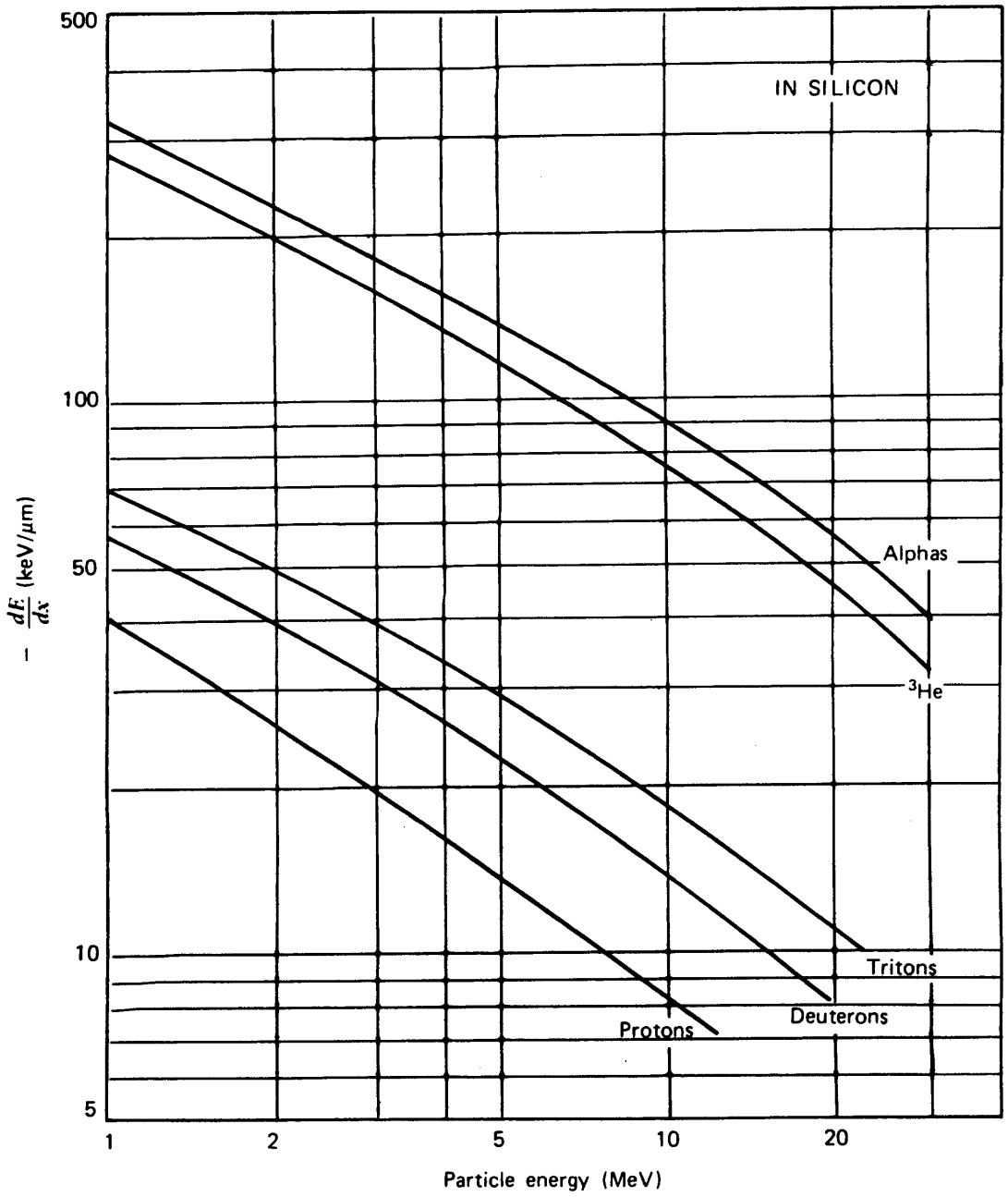

dE/dx for light to heavy charged particles in Al
(nearly the same in Si)

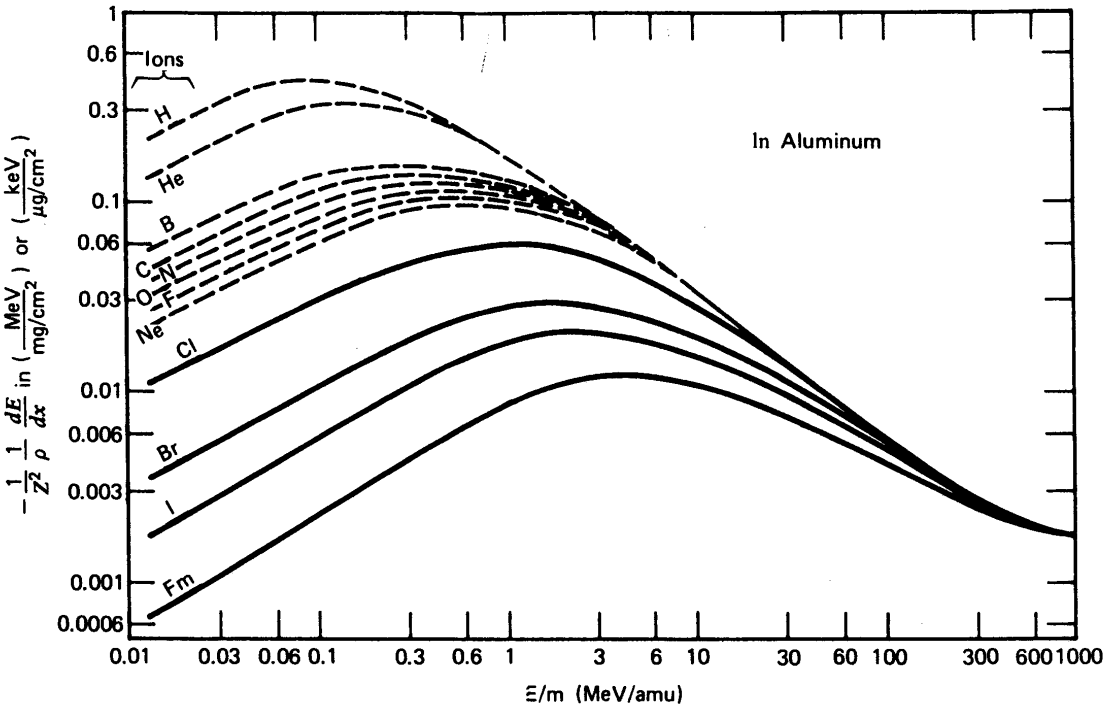

(from Northcliffe and Schilling, Nucl. Data Tables A7 (1970) 233)

Note that the vertical scale is normalized to Z^2 and density ρ.

In contrast to particles of low atomic number, the specific energy loss of heavy particles initially increases with energy. With increasing velocity, orbital electrons are stripped from the nucleus, thereby increasing the effective charge of the projectile. Beyond the peak dE/dx, where the projectiles are fully stripped, the specific ionization falls as predicted by the Bethe-Bloch formula and attains minimum ionization at 1 GeV/amu.

Charged particles have a well-defined range (stopping distance)

Range-Energy curves for various charged particles in Si

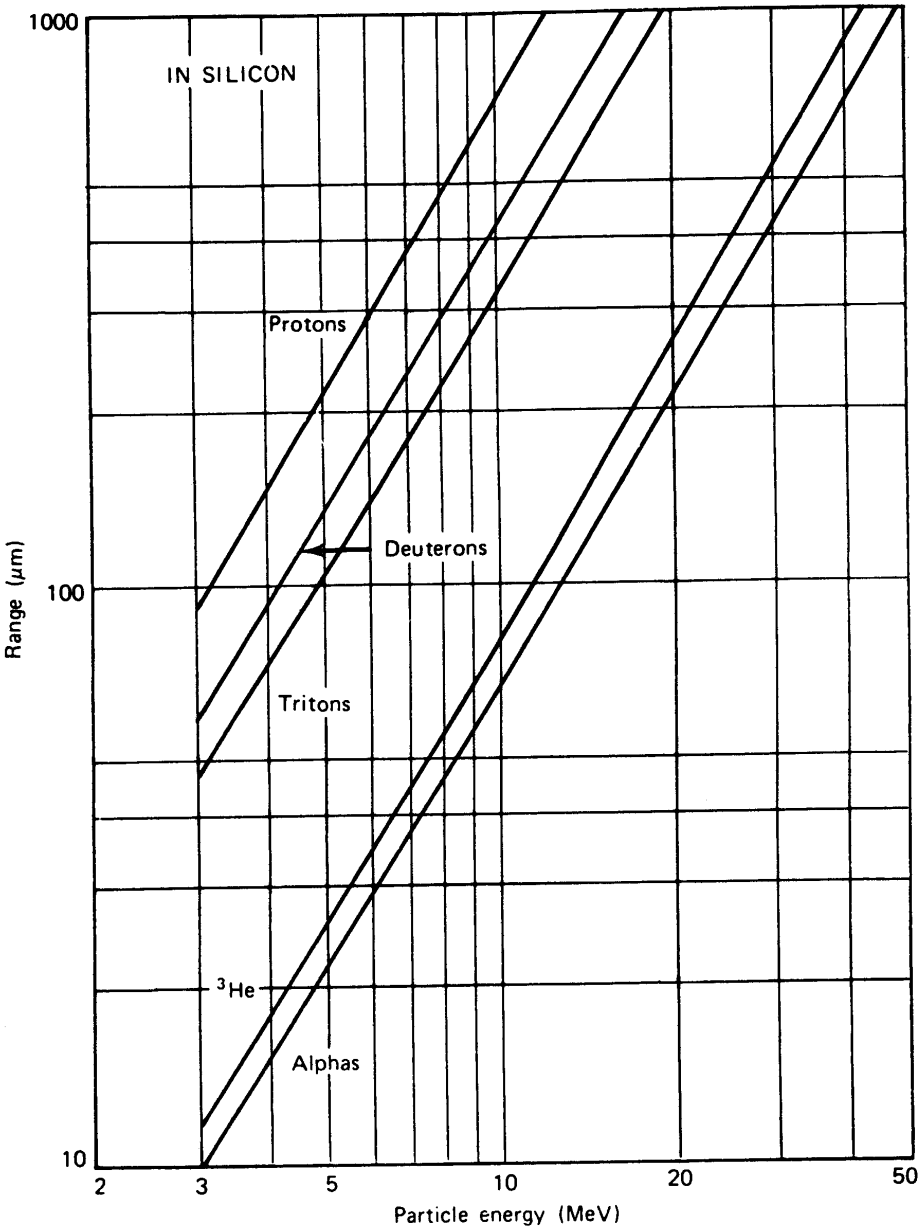

Towards the end of their range the specific energy loss of charged particles increases and they move more slowly, depositing even more energy per unit distance.

$\Rightarrow$ "Bragg Peak"

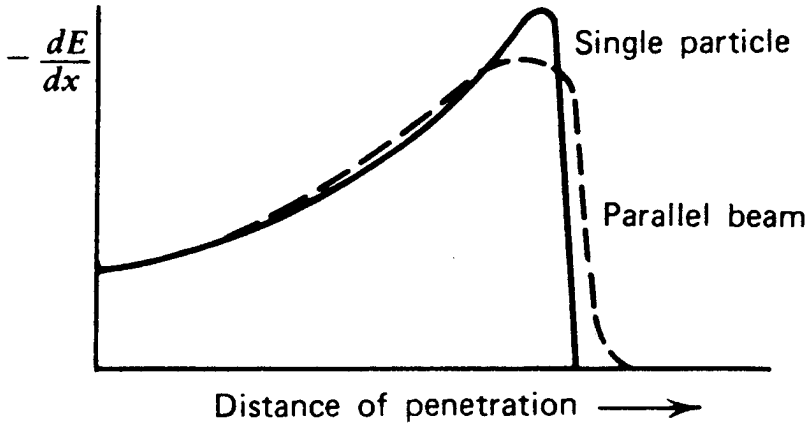

For a beam of particles the Bragg peak is smeared because of multiple scattering.

At low energies the range of particles decreases drastically with increasing projectile charge.

For E = 5 MeV in Si:	p	R = 220 μm
	α	R = 25 μm
	^{16}O	R = 4.3 μm
	^{40}Ca	R = 3.0 μm
	^{132}Xe	R = 2.0 μm
	^{197}Au	R = 1.4 μm

Energy Loss of Neutrons

Cross section much smaller.

Energy deposition due to knock-on collisions that displace absorber atoms, which deposit energy as charged particles.

Maximum recoil energy transferred to a nucleus of mass number A for head-on collision

$$E_{\max} = \frac{4A}{(A+1)^2} E_n$$

Maximum for protons ($E_{max} = E_n$), whereas for C $E_{max} = 0.35\ E_n$

Hydrogenous absorber most effective as neutron detectors

$\Rightarrow$ plastic scintillators

For fast neutrons up to 10 MeV the scattering is isotropic, so the energy distribution of the recoil protons is uniform from $E_p = 0$ to $E_p = E_n$.

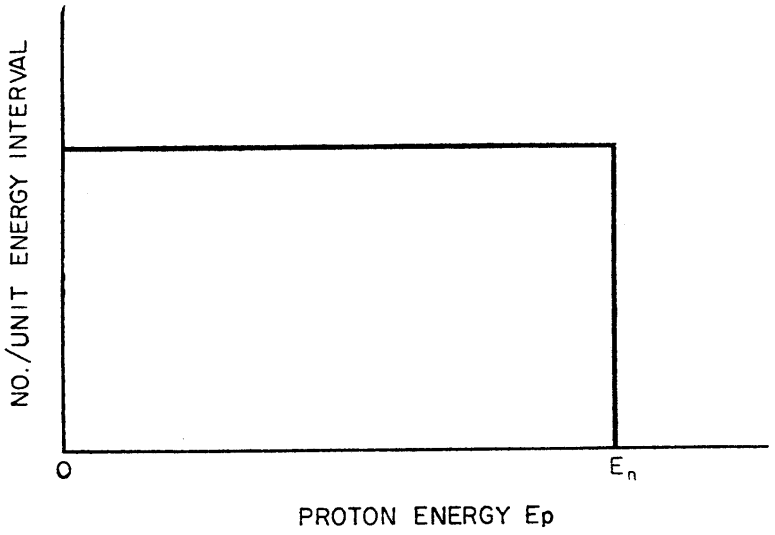

Except for very low energy photons, the spectrum provided by plastic scintillators is dominated by Compton scattering.

Interactions of Gamma Rays

In contrast to charged particles, which deposit energy continuously along their track, photon interactions are localized.

In passing through a medium, photons will traverse a certain distance unaffected, until depositing energy either by

a) photoelectric absorption

b) Compton scattering

c) pair production

The probability of undergoing an interaction is an exponential function of distance. The fraction of photons that suffered any interaction after traversing a distance x is

$$f = 1 - \exp(-\mu x)$$

where μ is a linear absorption coefficient, expressed in cm^{-1}, which is the sum of the individual absorption coefficients of the relevant interactions.

The absorption can be parameterized more generally by the mass attenuation coefficient μ/ρ, expressed in cm^2g^{-1}, which is independent of the density or physical state of the absorber.

For a mixture of elements of weight fractions w_i the composite mass attenuation coefficient is

$$\frac{\mu}{\rho} = \frac{\mu_1}{\rho_1} w_1 + \frac{\mu_2}{\rho_2} w_2 + \ ....$$

a) Photoelectric Absorption

Photon deposits its total energy in a single interaction with an absorber atom.

A photoelectron is emitted with the energy

$$E_e = E_\gamma - E_b$$

where E_b is the binding energy of the photoelectron.

Photoelectric absorption dominates at rather low energies, but the cross section increases rapidly with Z.

$$\sigma_{pe} \propto \frac{Z^n}{E_\gamma^{3.5}}$$

where n varies from 4 to 5.

At energies and absorber atomic numbers where this process is important, the photoelectron typically is absorbed within a short distance, so the total energy is registered in the detector.

X-rays emitted by the decay of the ionized atom to its ground state are also absorbed in the detector.

$\Rightarrow$ measured spectrum

b) Compton Scattering

Photon scatters off of an electron.

$\Rightarrow$ photon deflected with decreased energy

$$E_\gamma ' = \frac{E_\gamma}{1+\alpha(1-\cos\Theta)}$$

where

$$\alpha \equiv E_\gamma \ / \ m_0 c^2$$

Relative number of photons Compton scattered per unit solid angle vs. scattering angle Θ and initial photon energy.

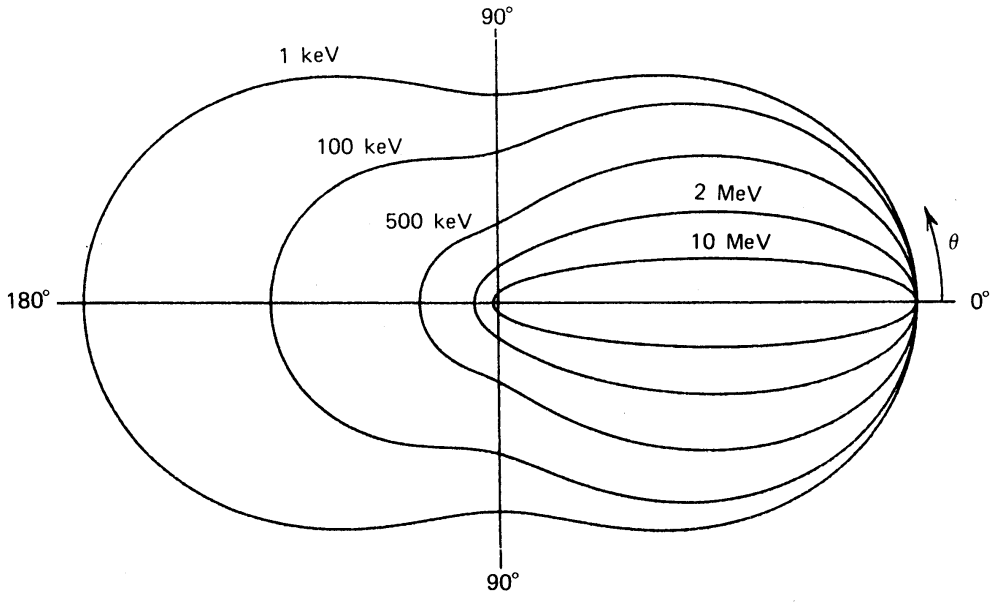

The primary photon is incident from the left.

At higher energies photons scattered near the far boundary of the detector will tend to escape from the detector, leading to a deficit in the measured energy.

Recoil electron emitted with energy up to a maximum value

$$T_{cm} = \frac{E_\gamma}{1 + (1/2\alpha)} \ ,$$

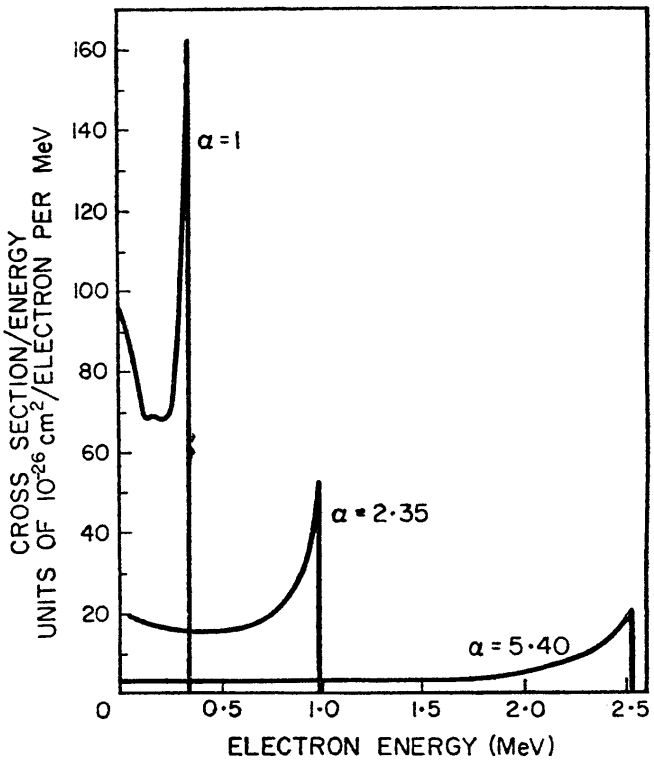

If the scattered photon exits the sensitive volume of the detector without interaction, the electron energy spectrum is what will be registered by the detector.

Electron scattering at $\Theta = \pi$ imposes an upper bound on the energy of the scattered photon

$$E_C = E_\gamma - E_{el}|_{\Theta=\pi} = \frac{E_\gamma}{1 + 2E_\gamma / m_0 c^2} \ ,$$

the “Compton edge”.

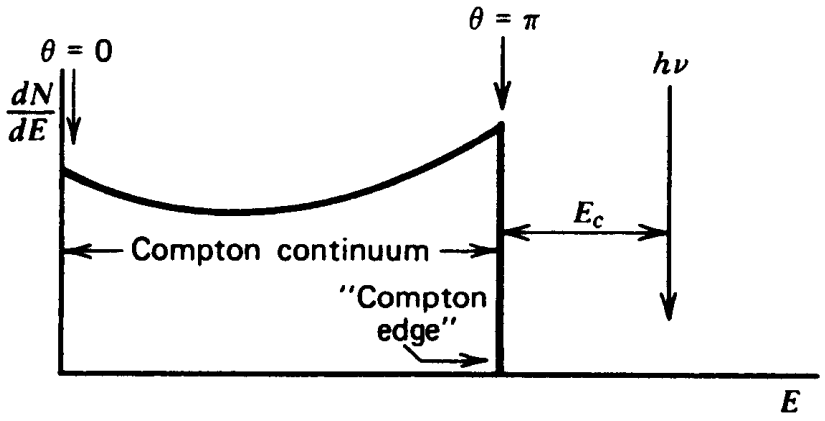

For large photon energies E_γ this energy converges toward a constant value, placing the Compton edge below the primary photon peak by

$$E_C(E_\gamma \to \infty) = \frac{m_0 c^2}{2} = 256 \text{ keV}$$

c) Pair Production

If the photon energy is twice the mass of the electron, electron-positron pairs can be produced.

No simple expression for the cross section vs. energy, but this process becomes significant at photon energies above several MeV.

The excess photon energy beyond $2m_0c^2$ goes into kinetic energy shared between the electron and positron.

The positron can interact within the detector yielding two 511 keV annihilation photons

If these are absorbed in the detector, the measured energy spectrum is

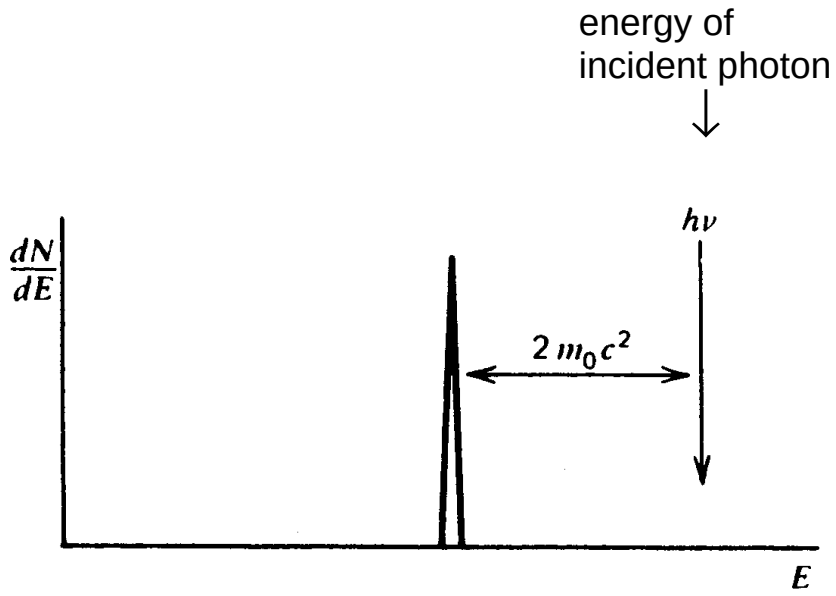

Absorption Processes vs. Energy in NaI(Ti)

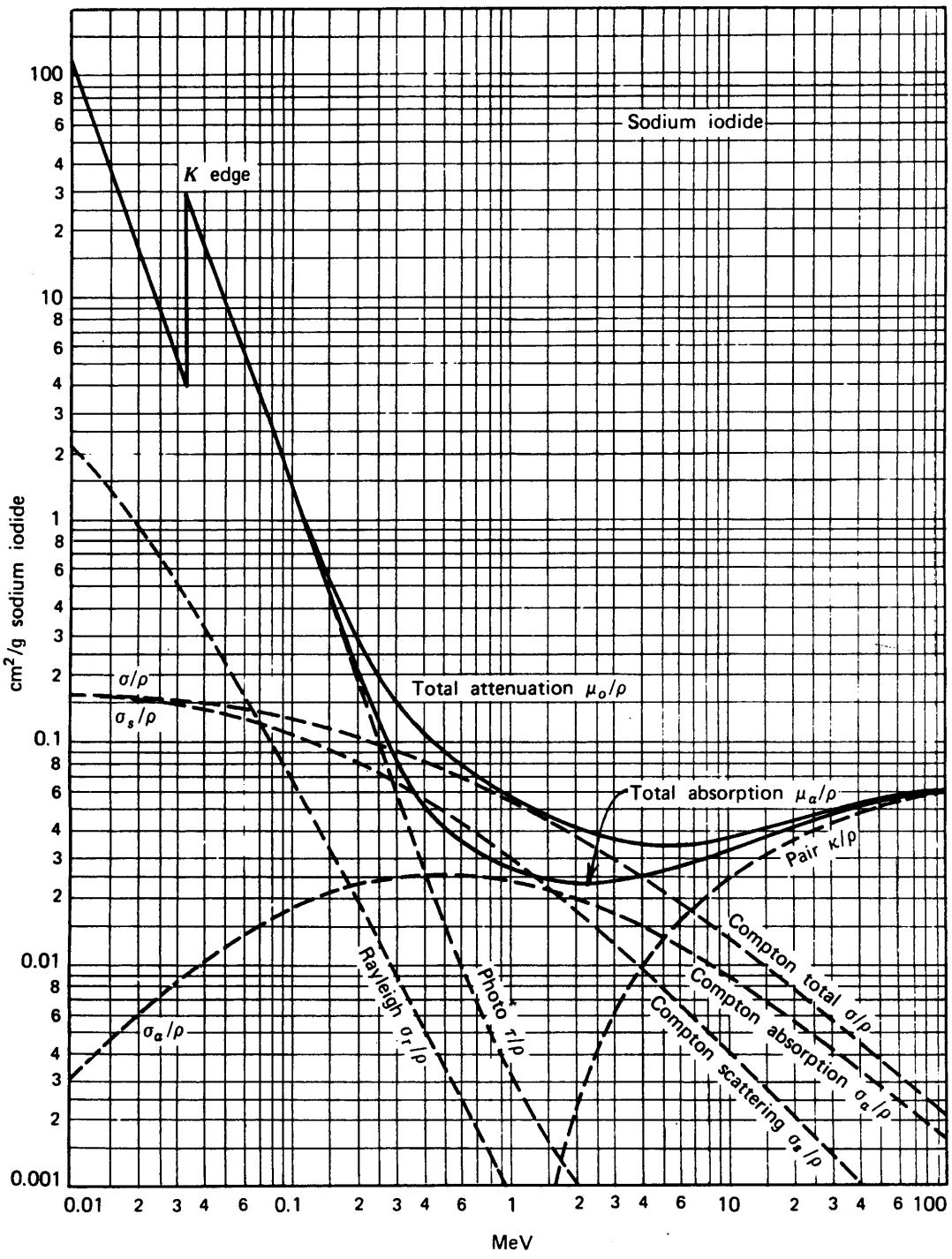

Relative importance of the three major type of gamma-ray interactions vs. energy and atomic number Z of the absorber.

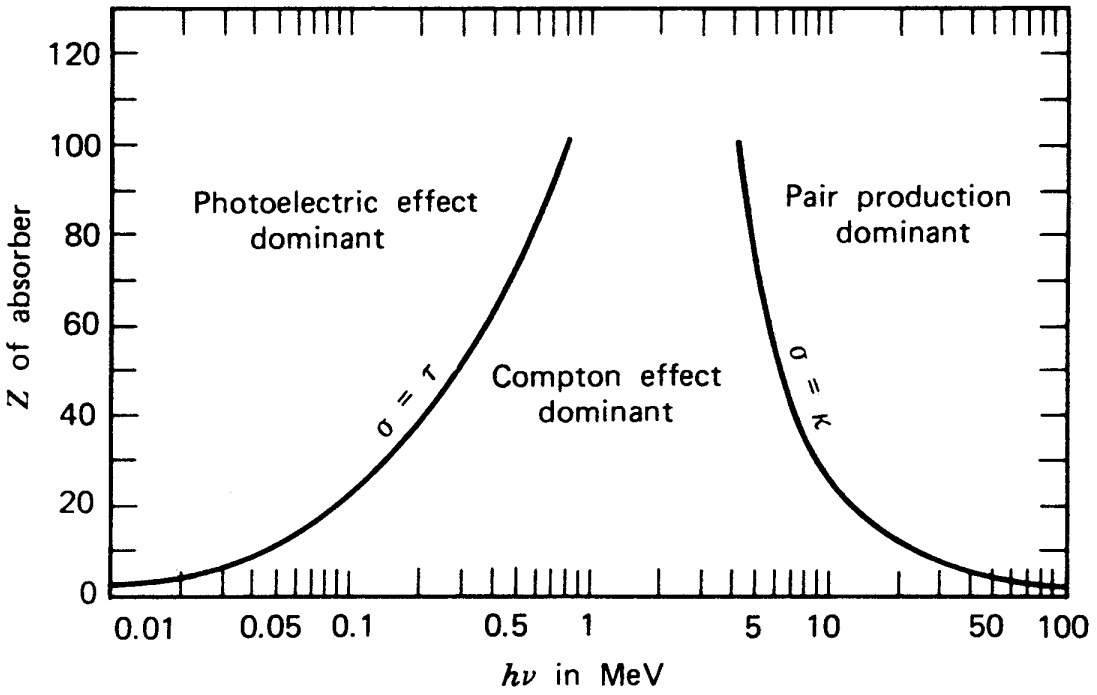

(from Knoll)

The lines show the values of Z and $E_\gamma = h\nu$ where the two neighboring are equal.

Implications for Required Detector Size

Linear absorption coefficient for Si:

For N_0 incident photons photons impinging on a medium, the number that traverse the length x without interaction is

$$N = N_0 e^{-\sigma_L x}$$

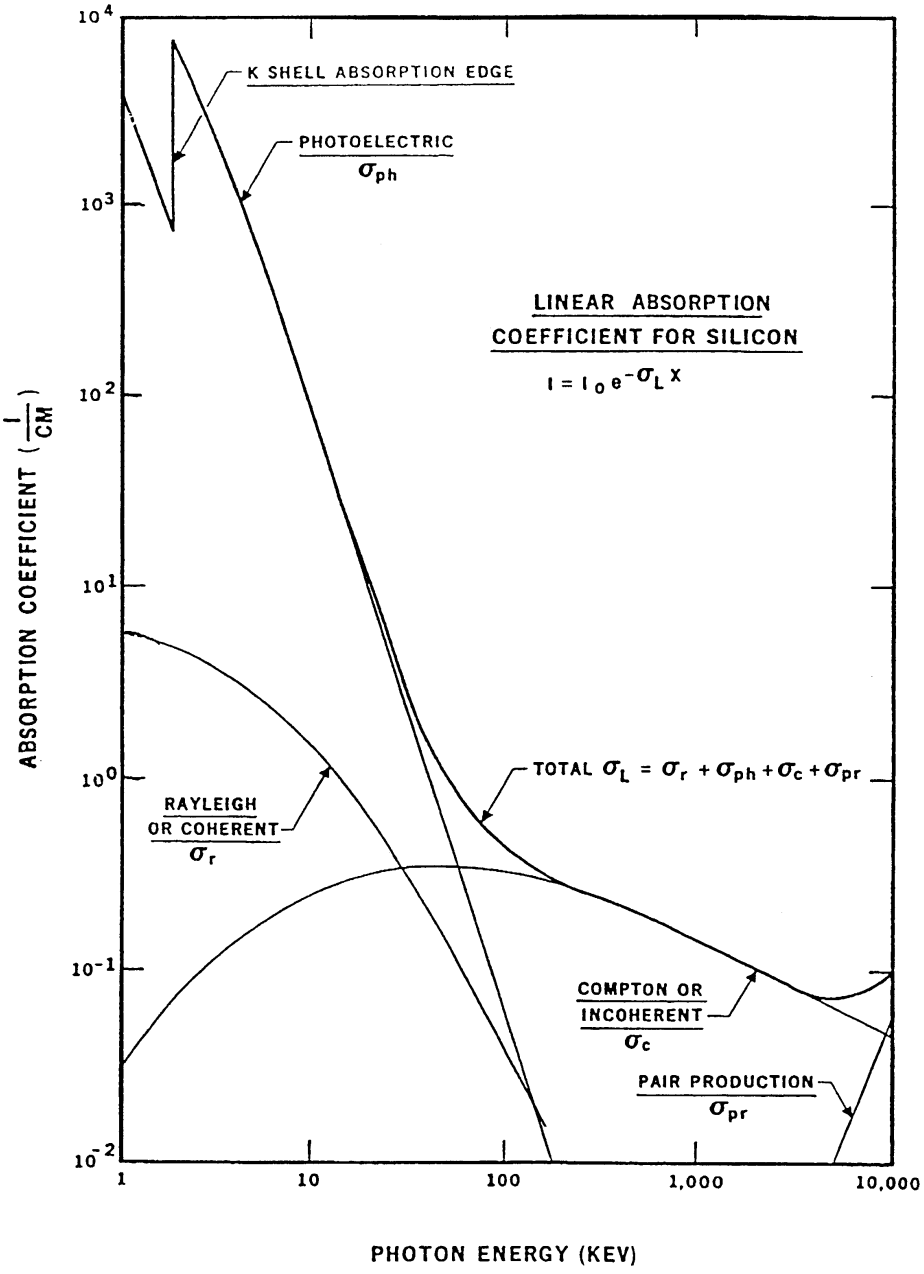

For example, the absorption of 10 keV photons in Si is dominated by the photoelectric effect with $\sigma_{ph} \approx 10^2$ cm^{-1}. If a detector is 300 μm thick, i.e. $\sigma_{ph} x \approx 3$, then 95% of the photons will interact in the detector. Since the range of the emitted photoelectron is about 1 μm, all of the primary energy is absorbed in the detector volume.

The absorption coefficient decreases rapidly with energy.

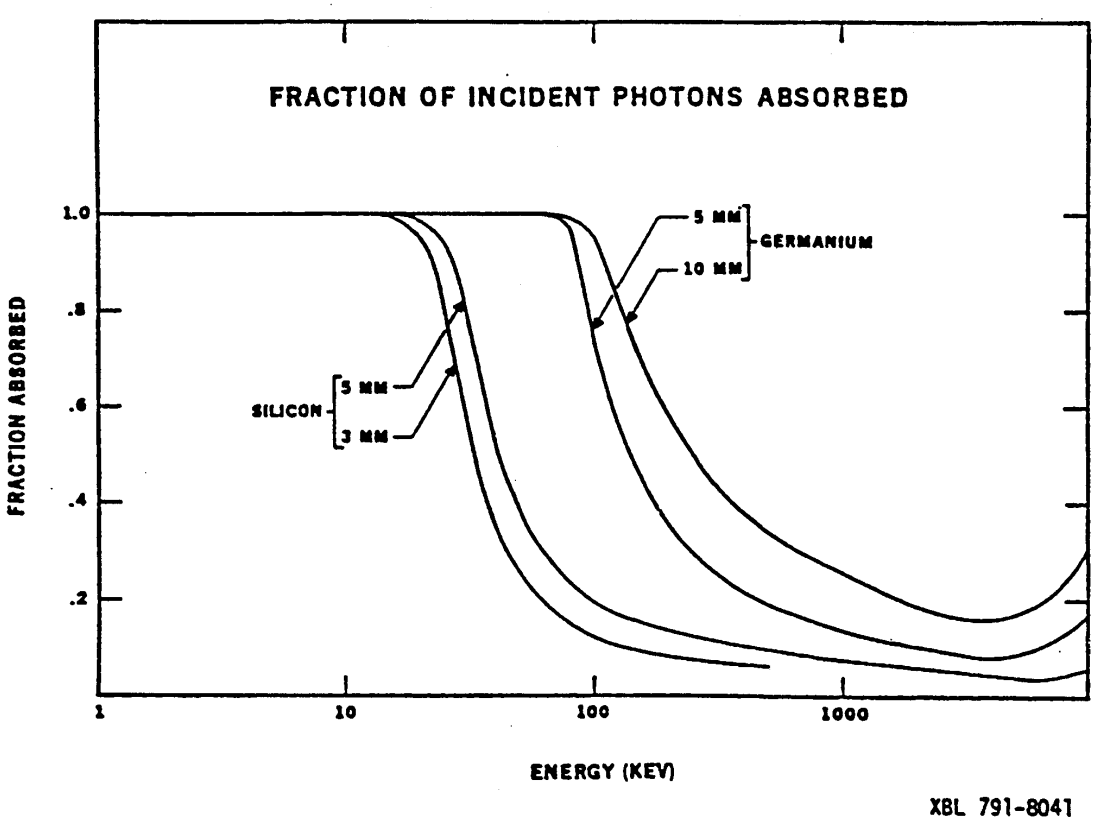

For a photon of 1 MeV, practically all absorption in Si is due to Compton scattering with an absorption coefficient $\sigma_c \approx 10^{-1}$ cm^{-1}. In a 300 μm thick detector, only 0.3% will interact. For 95% absorption, the detector must be 30 mm thick. Even then, the scattered photon may still leave the absorber without further interaction, so only a fraction of the primary photon energy remains in the detector. For full energy absorption with good efficiency the detector would have to be made even larger.

The alternative is to use a material with larger atomic number Z. As shown in the previous graph, Ge maintains high efficiency to higher energies than a Si absorber of the same size.

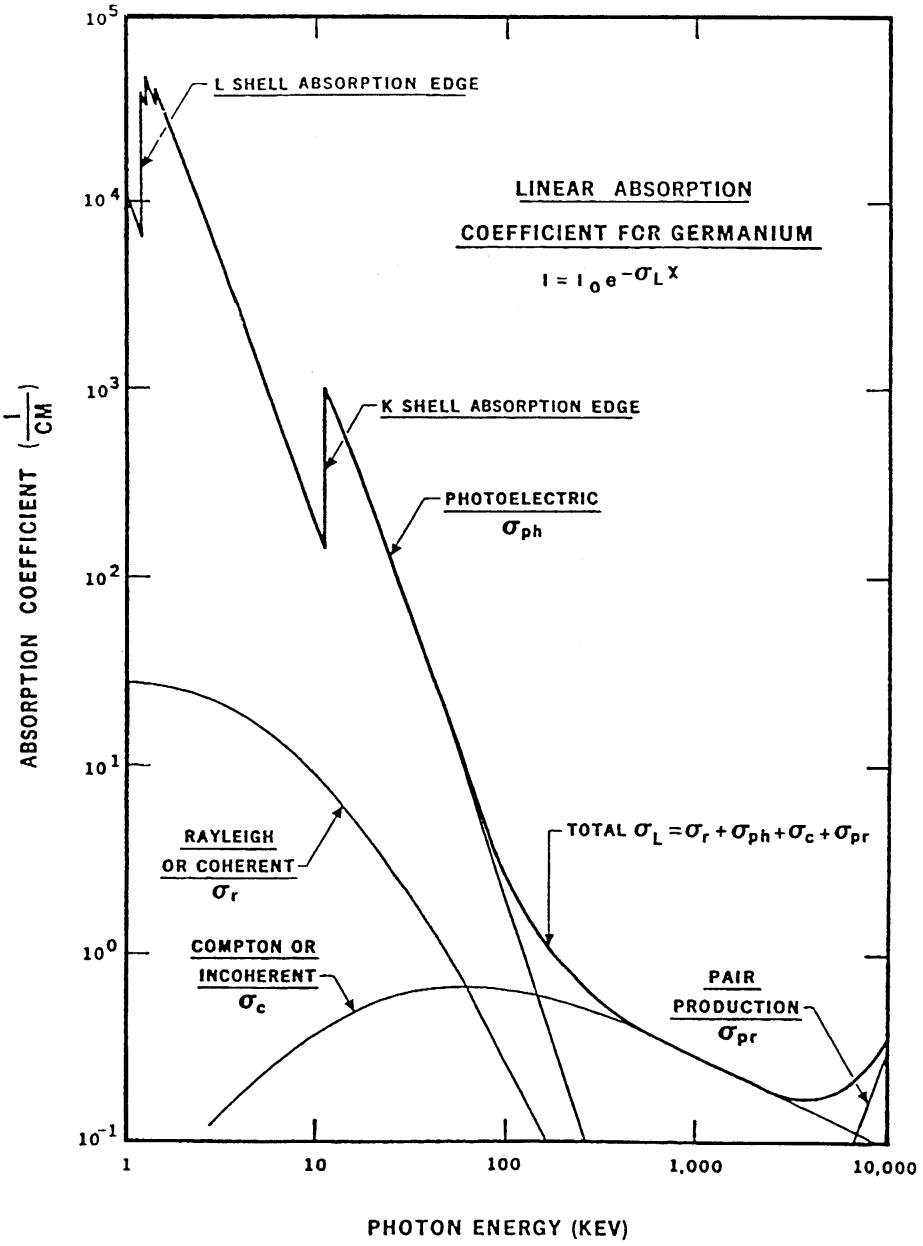

At higher energies the required crystal volume for Si or Ge becomes impractical or prohibitively expensive, so higher Z materials become attractive, for example $NaI(Tl)$, where iodine (Z= 53) is the primary absorber, or Bismuth-Germinate ($Bi_4Ge_3O_{12}$, “BGO”), where Bismuth (Z= 83) provides even higher absorption efficiency.

Energy Spectra for various Detector Sizes
(adapted from Knoll)

a) Large Detector

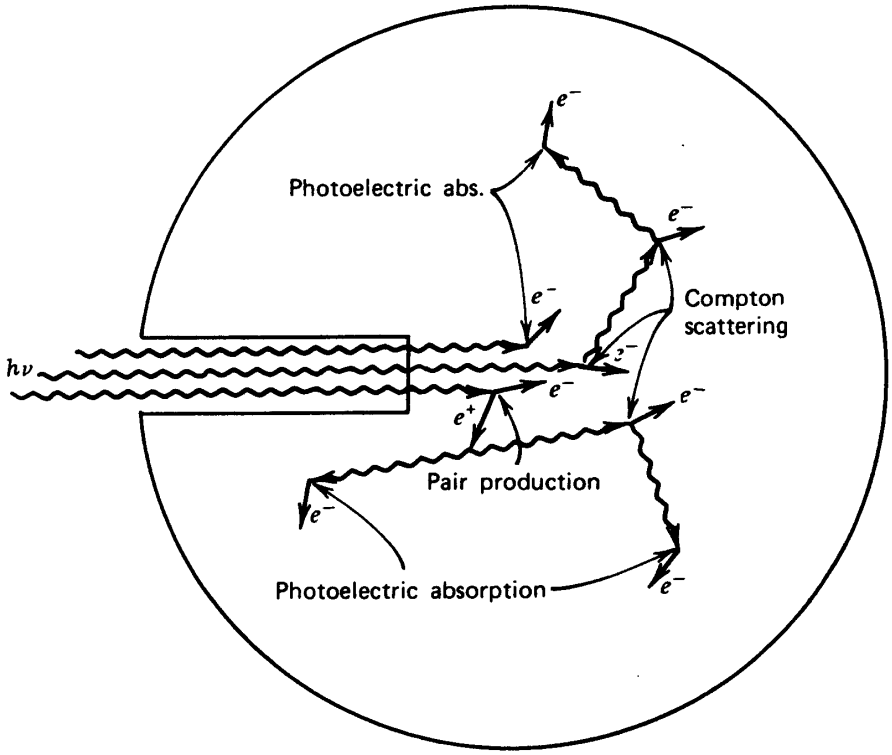

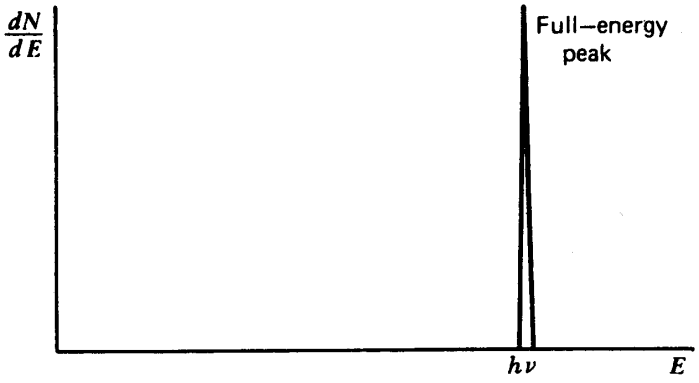

All secondaries absorbed.

b) Small Detector

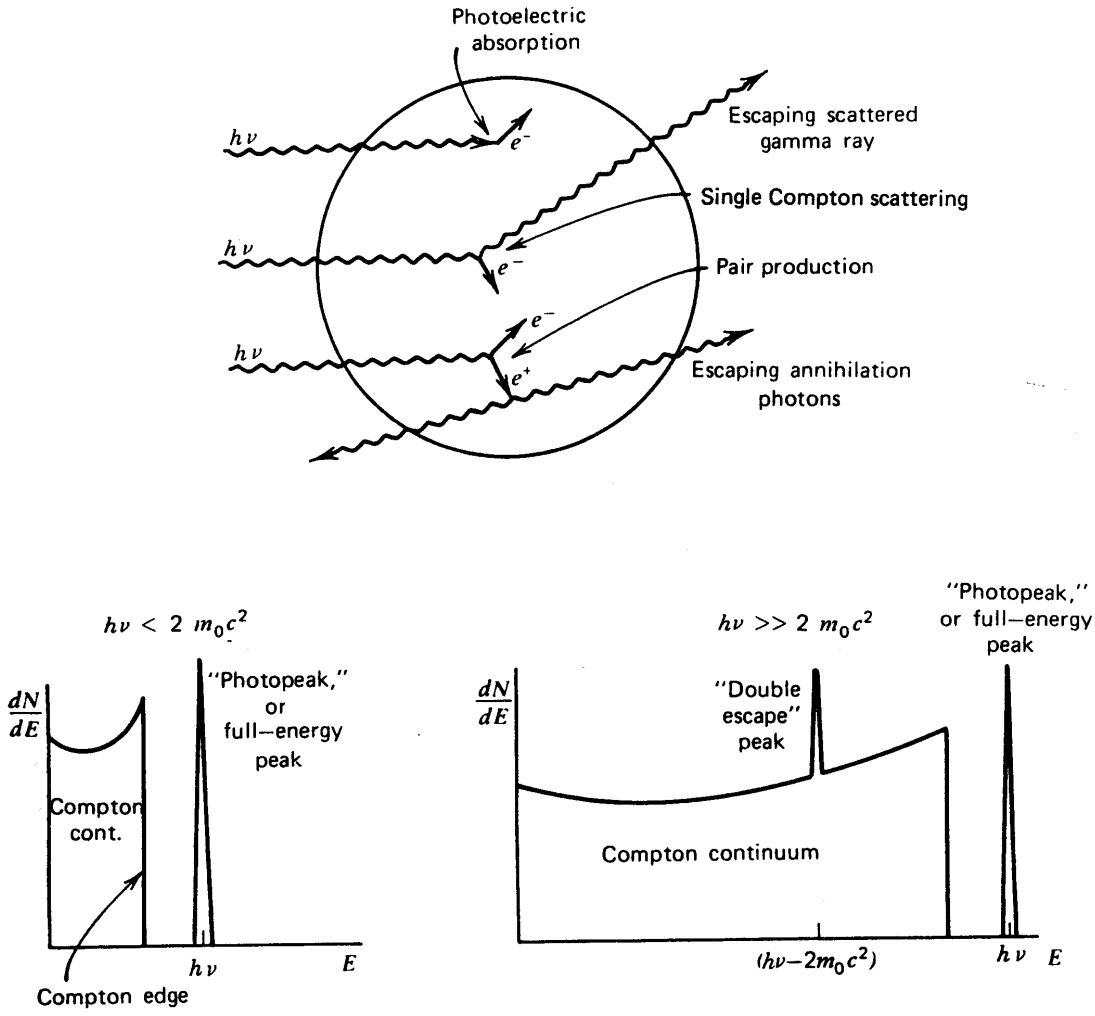

In the small detector there is a substantial probability that neither the Compton scattered gamma nor the two 511 keV annihilation photons from pair production are registered in the detector.

c) Intermediate Volume Detector

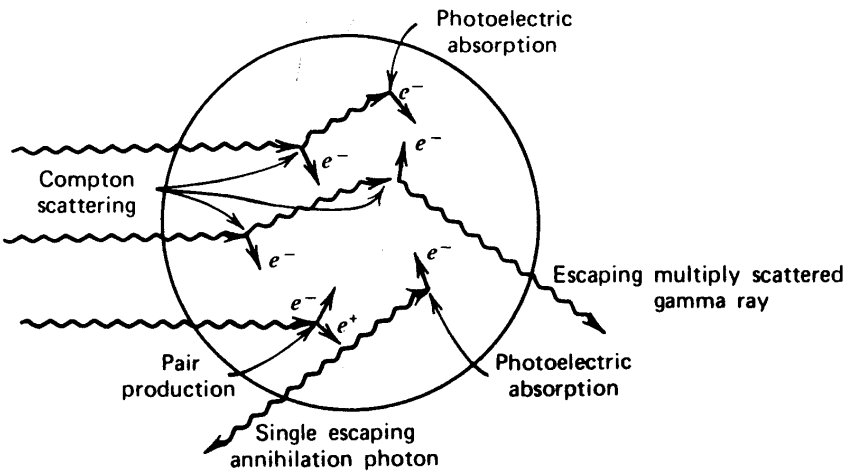

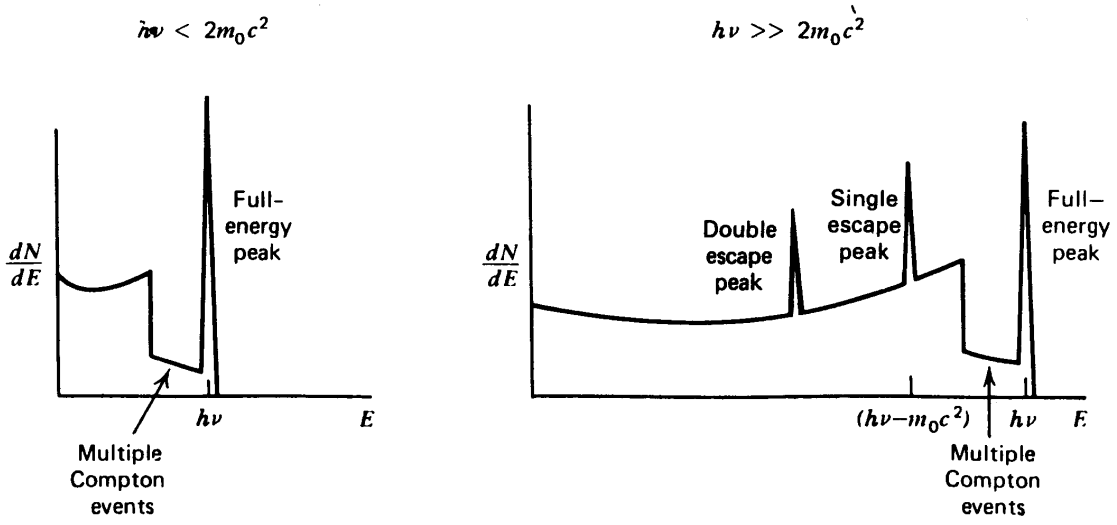

In the intermediate volume detector the initial Compton-scattered photon can scatter again with escape of the final scattered photon.

⇒ energy deposition above Compton edge

One annihilation photon from pair-production is absorbed and one escapes

⇒ “single escape peak”

d) Effect of Surrounding Material

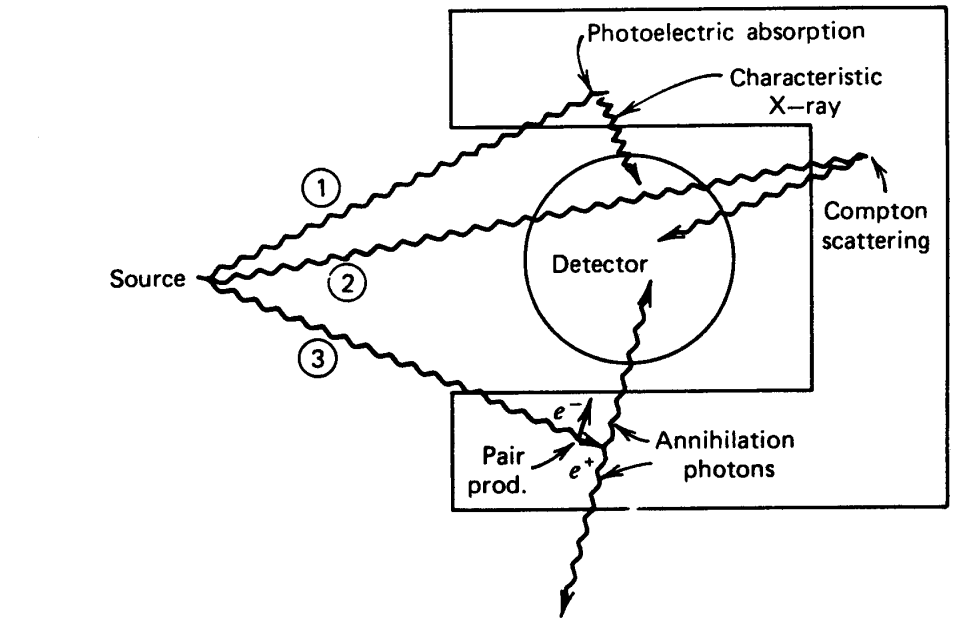

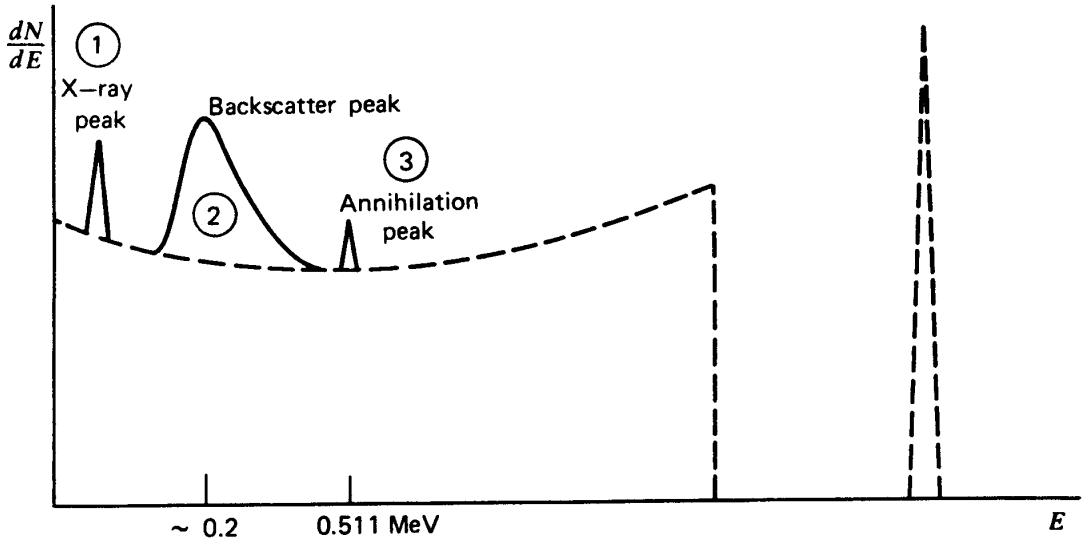

(1) x-ray from photoelectric absorption in external material

(2) Compton backscatter peak (see next page)

(3) Absorption of one 511 keV annihilation photon from pair-production in external material.

Compton Backscattering

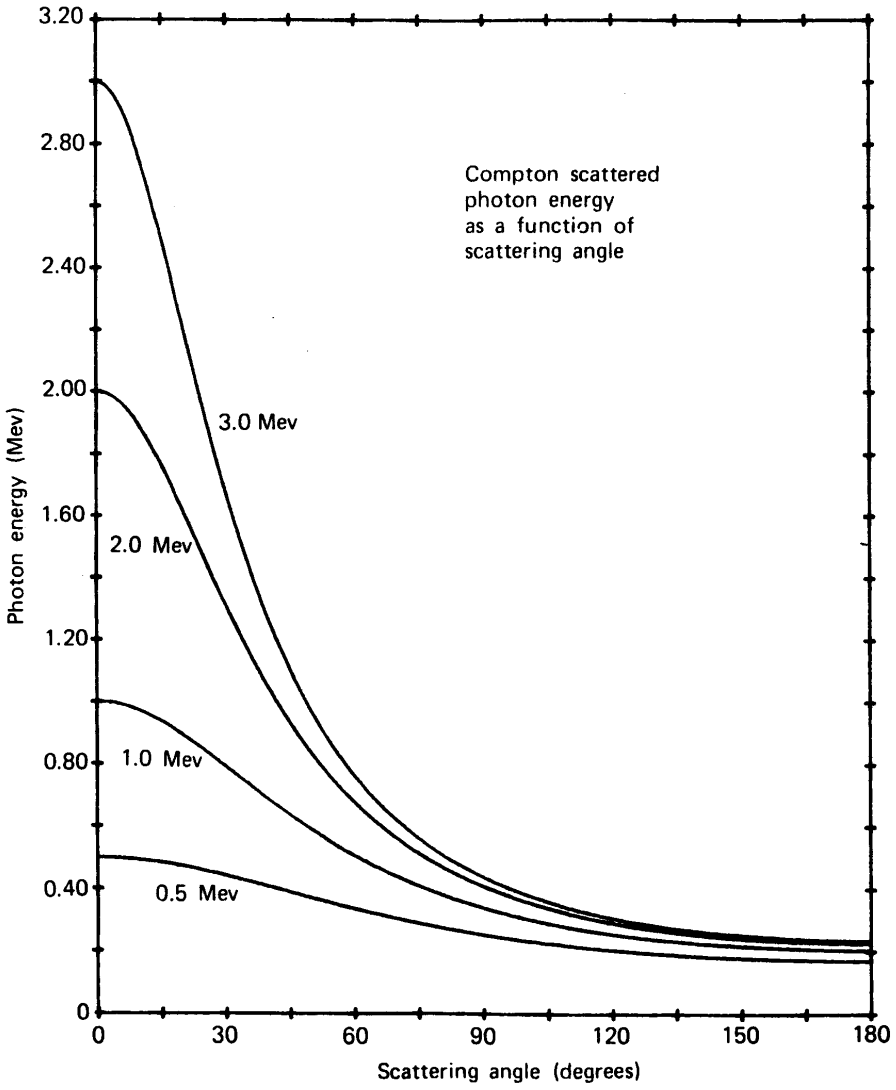

At 180° all incident photon energies yield a narrow energy distribution of the scattered photon ("backscatter peak").

Example for scintillation detector with particle ID using dE/dx

Plastic Ball Detector

A. Baden, H.H. Gutbrod, H. Löhner, M.R. Maier, A.M. Poskanzer, T. Renner, H. Riedesel, H.G. Ritter, H. Spieler, A. Warwick, F. Weik, and H. Wieman, NIM **203** (1982) 189

Use two scintillators ("phoswich")

CaF_2(Eu)	slow decay
Plastic	fast decay

Thin CaF_2(Eu) scintillator uses long plastic scintillator as a light guide.

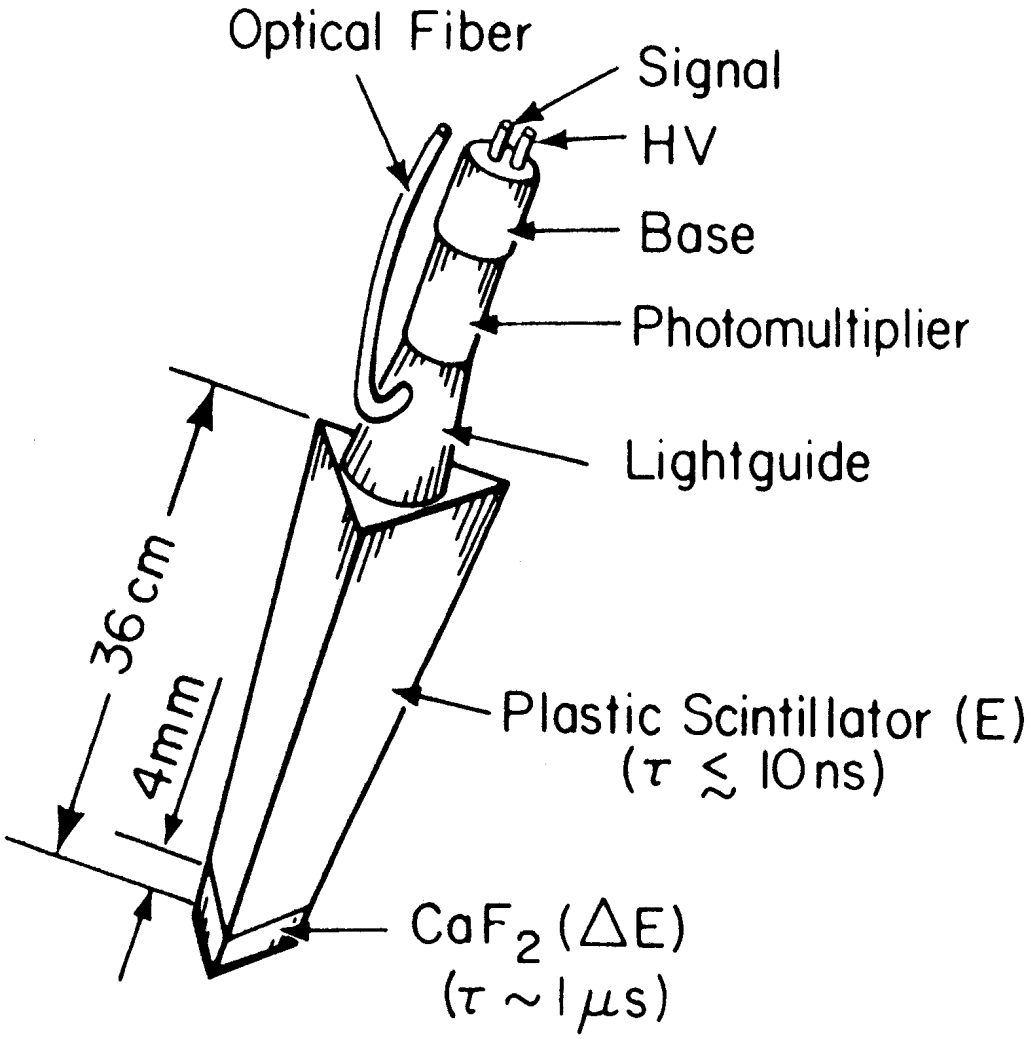

Two integrating ADCs are used.

One with a short gate to measure the fast light output from the plastic, the second with a long gate to measure the light from the CaF_2.

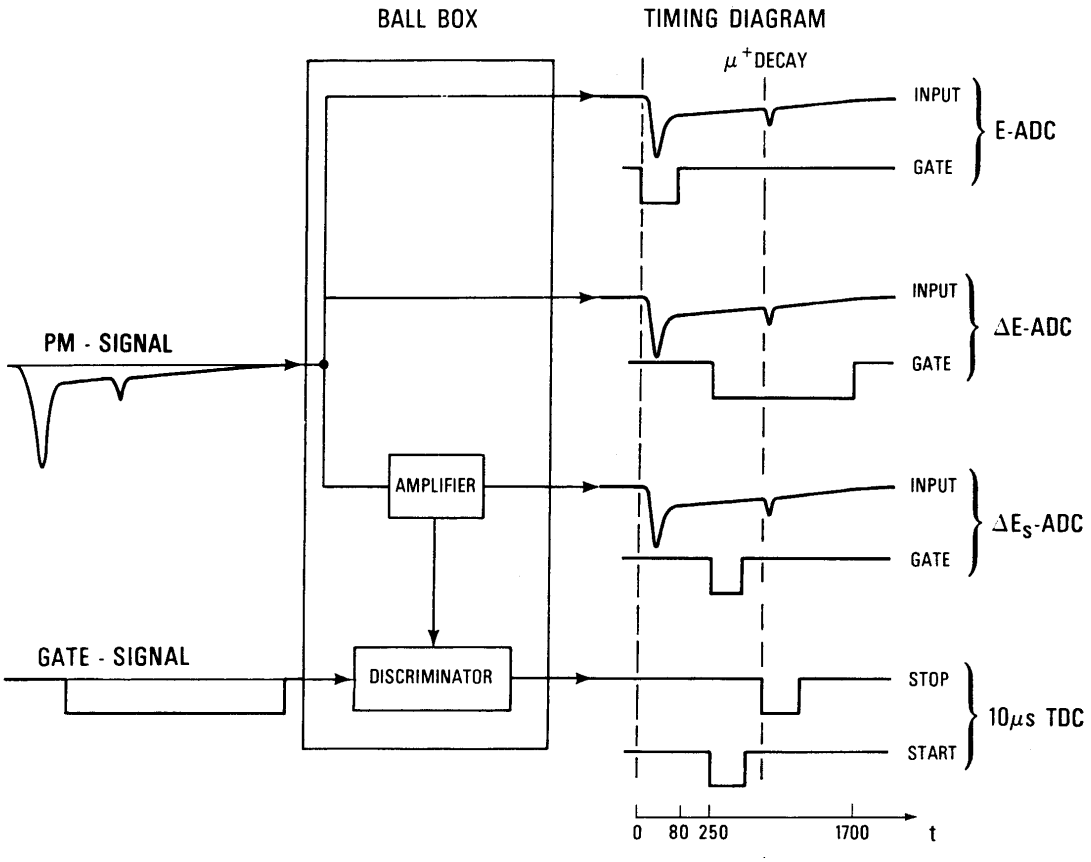

π+ tend to disappear in strong background, so additional identification applied.

π^+ lifetime 26 ns: $\pi^+ \rightarrow \mu^+ + \nu$

μ^+ lifetime 2.2 μs : $\mu^+ \rightarrow e^+ + 2\nu$

e^+ emitted with energy up to 53 MeV and easily detected in plastic scintillator.

Particle ID Characteristics

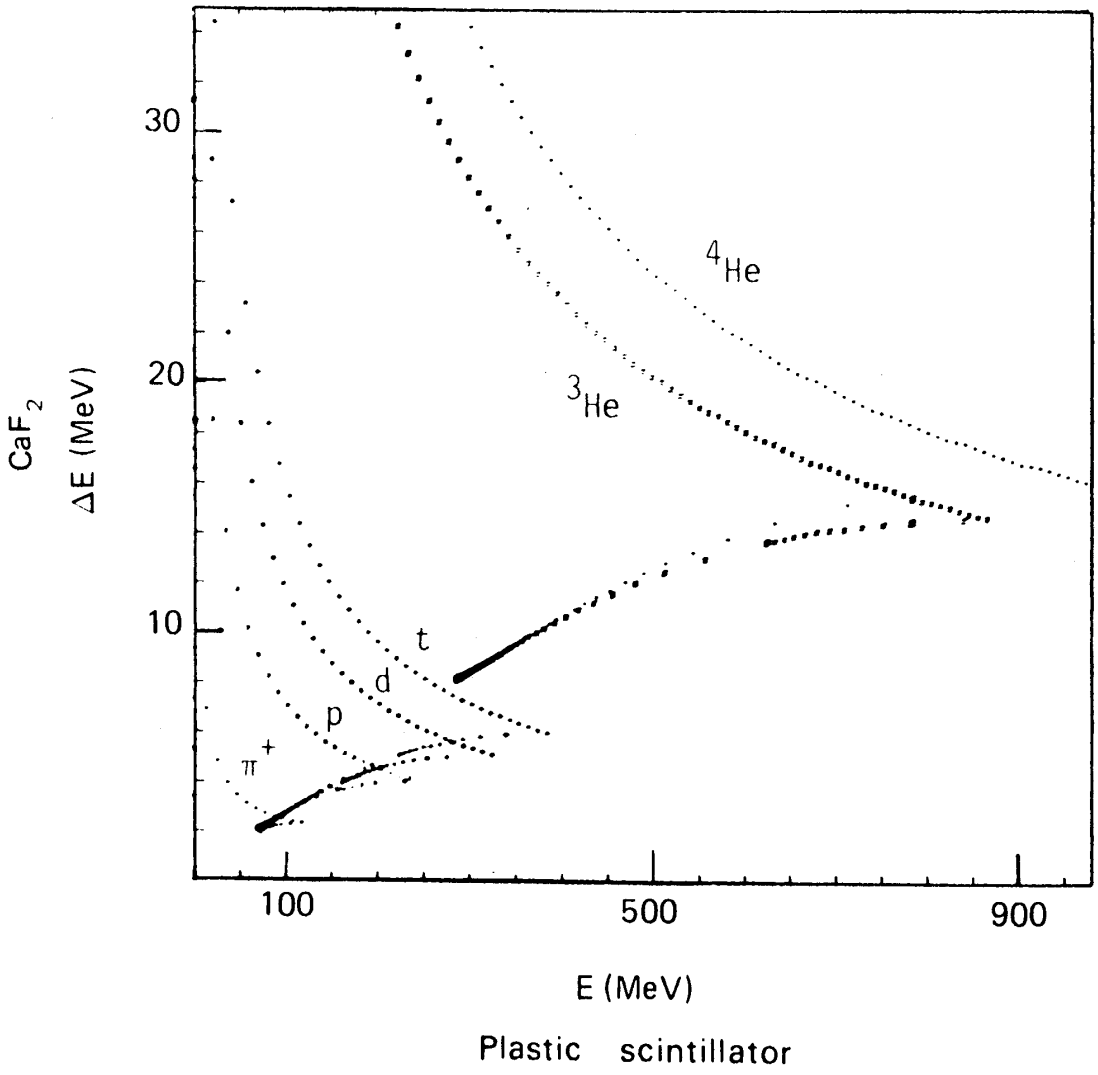

Comparison between γ spectra taken with NaI(Tl) scintillator and Ge semiconductor detector

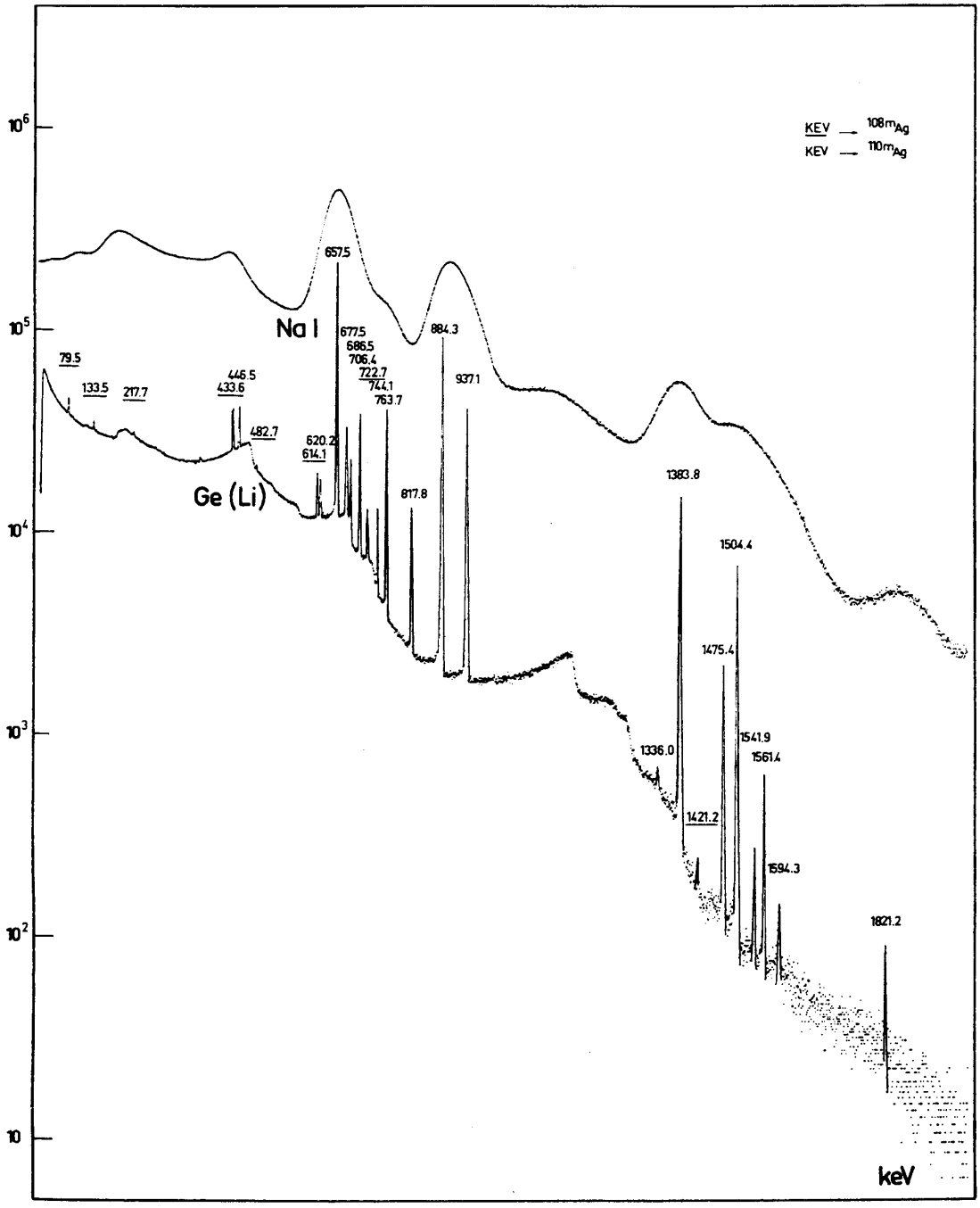

(J.Cl. Philippot, IEEE Trans. Nucl. Sci. NS-17/3 (1970) 446)

Semiconductor detectors provide much better resolution than scintillators.